TECHNICAL REPORT
NATICK/TR-93/029

AD_____

A COMPUTATIONAL MODEL THAT COUPLES AERODYNAMIC AND STRUCTURAL DYNAMIC BEHAVIOR OF PARACHUTES DURING THE OPENING PROCESS

By
Keith R. Stein
Richard J. Benney
Earl C. Steeves

April 1993

FINAL REPORT
October 1991 to January 1993

UNITED STATES ARMY NATICK
RESEARCH, DEVELOPMENT AND ENGINEERING CENTER
NATICK, MASSACHUSETTS 01760-5000

AERO-MECHANICAL ENGINEERING DIRECTORATE

DISCLAIMERS

The findings contained in this report are not to be construed as an official Department of the Army position unless so designated by other authorized documents.

Citation of trade names in this report does not constitute an official endorsement or approval of the use of such items.

DESTRUCTION NOTICE

For Classified Documents:

Follow the procedures in DoD 5200.22-M, Industrial Security Manual, Section II-19 or DoD 5200.1-R, Information Security Program Regulation, Chapter IX.

For Unclassified/Limited Distribution Documents:

Destroy by any method that prevents disclosure of contents or reconstruction of the document.

REPORT DOCUMENTATION PAGE

Form Approved
OMB No 0704-0188

1. AGENCY USE ONLY (Leave blank)	2. REPORT DATE	3. REPORT TYPE AND DATES COVERED
	April 93	Final October 91 to January 93

4. TITLE AND SUBTITLE

A COMPUTATIONAL MODEL THAT COUPLES AERODYNAMIC AND STRUCTURAL DYNAMIC BEHAVIOR OF PARACHUTES DURING THE OPENING PROCESS

5. FUNDING NUMBERS

PR: 1L162786D283,
1L162786D283,
1L161102AH52
PE: 62786D, 62786D, 61102A
WU: H00, A00, B00
TA: AJ, AF, 02
AG: T/B 1347, T/B 1427, T/B 1344

6. AUTHOR(S)

KEITH R. STEIN, RICHARD J. BENNEY, EARL C. STEEVES

7. PERFORMING ORGANIZATION NAME(S) AND ADDRESS(ES)

U.S. Army Natick RD&E Center
ATTN: SATNC-UE
Natick, MA 01760-5017

8. PERFORMING ORGANIZATION REPORT NUMBER

NATICK/TR-93/029

9. SPONSORING / MONITORING AGENCY NAME(S) AND ADDRESS(ES)

10. SPONSORING / MONITORING AGENCY REPORT NUMBER

11. SUPPLEMENTARY NOTES

12a. DISTRIBUTION AVAILABILITY STATEMENT

Approved for public release; distribution unlimited

12b. DISTRIBUTION CODE

13. ABSTRACT *(Maximum 200 words)*

In parachute research, the canopy inflation process is the least understood and most complex to model. Unfortunately, it is during the opening process that the canopy often experiences the largest deformations and loadings. The complexity of modelling the opening process stems from the coupling between the structural dynamics of the canopy, lines and payload with the aerodynamics of the surrounding fluid medium. The addition of a computational capability to model the coupled opening behavior would greatly assist in the understanding of the canopy inflation process. Ongoing research at the U.S. Army Natick Research, Development and Engineering Center (Natick) focuses on this coupled problem. The solution to the coupled problem is expected to assist in the development of future U.S. Army airdrop systems which include the capability of deploying at low altitudes and high speeds. A computational fluid dynamics (CFD) code and structural dynamic mass spring damper (MSD) code are coupled with an explicit marching method. The CFD flow solver provides the differential pressure values at node points along a radial which are used as input in the MSD model. The MSD code integrates the equations of motion for the canopy and returns current nodal positions and velocities to the CFD code. The node points on the MSD model coincide with a unique set of adjacent CFD grid points for all time. This coupled model predicts behavior for a quarter-scale C-9 parachute which compares favorably with experimentally determined behavior.

14. SUBJECT TERMS		15. NUMBER OF PAGES
COMPUTATIONAL FLUID DYNAMICS	PARACHUTE MODELS AERODYNAMIC CHARACTERISTICS	33
MASS SPRING DAMPING SYSTEM	STRUCTURAL ANALYSIS	16. PRICE CODE
FLUID-STRUCTURE INTERACTION	PARACHUTE OPENING	

17. SECURITY CLASSIFICATION OF REPORT	18. SECURITY CLASSIFICATION OF THIS PAGE	19. SECURITY CLASSIFICATION OF ABSTRACT	20. LIMITATION OF ABSTRACT
UNCLASSIFIED	UNCLASSIFIED	UNCLASSIFIED	SAR

CONTENTS

FIGURES

FIGURES (cont'd)

PREFACE

This report describes the efforts undertaken as part of the project T/B1347 "Computational Prediction of the Optimum Shape for Aerodynamic Decelerators", using Project 1L162786D283AJHOO funds; T/B1427 "Nonlinear Structural Dynamic Behavior of Parachutes", using Project 1L162786D283AFA00 funds; "Computational Fluid Dynamics for Parachute Opening", using Project 1L161102AH5202BOO funds. This effort was undertaken during the period October 1991 through December 1993. This work was performed by the Engineering Technology Division (ETD) of the Aero-Mechanical Engineering Directorate (AMED).

LIST OF SYMBOLS

A	cross sectional area of lines
Cm_i	meridional damping constant
E_1	Young's modulus of lines
E_2	Young's modulus of canopy fabric
g	gravitational constant
h	canopy fabric thickness
kh_i	hoop spring constant
km_i	meridional spring constant
lo_i	constructed meridional distance between mass points i and $i+1$
Δl_i	positive amount of stretch between mass points i and $i+1$
m_i	mass associated with mass point i
N	total number of gores
n	total number of mass points
n_x	width of CFD grid in cells
n_y	height of CFD grid in cells
P_i	current force from pressure differential acting on and normal to mass point i
Δr_i	current x-position minus constructed meridional length for mass point i
t	time
xo_i	constructed meridional length to mass point i
$x(i)$	current x location of mass point i
$y(i)$	current y location of mass point i
α_i	angle defining normal direction of mass point i
β_i	angle defining relative angle between mass points i and $i+1$
ϕ	$2\pi/N$

A COMPUTATIONAL MODEL THAT COUPLES AERODYNAMIC AND STRUCTURAL DYNAMIC BEHAVIOR OF PARACHUTES DURING THE OPENING PROCESS

SUMMARY

In parachute research, the canopy inflation process is the least understood and most complex to model. Unfortunately it is during the opening process that the canopy often experiences the largest deformations and loadings. The complexity of modeling the opening process stems from the coupling between the structural dynamics of the canopy, lines plus payload and the aerodynamics of the surrounding fluid medium. The addition of a computational capability to model the coupled opening behavior would greatly assist in understanding the canopy inflation process. Ongoing research at the U.S. Army Natick Research, Development and Engineering Center (Natick) focuses on this coupled problem. The solution to this problem will assist in the development of future U.S. Army airdrop systems, which include the capability of deploying at low altitudes and high speeds.

This paper describes research at Natick that currently involves coupling a computational fluid dynamics (CFD) code to a mass spring damper (MSD) parachute structural code. The model is described and results are presented. Initial computational results compare favorably with experimental data for a quarter-scale C-9. Future enhancements to the coupled model are discussed.

INTRODUCTION

The time-variant aerodynamic characteristics associated with the opening of a parachute are extremely complex to model. The complexity of the problem arises largely from the fact that the flow field is dependent on the canopy shape, which is itself dependent on the flow field. A correct model must include the coupled behavior of the structural dynamics of the parachute system with the aerodynamics of the surrounding flow field. A coupled model will provide not only information about the opening characteristics of a parachute but also characteristics of the parachute in its terminal velocity state including the parachute's shape, drag, velocity, pressure distribution, and flow-field characteristics.

Previously, either the aerodynamic or the structural dynamic behavior of the parachute opening problem was studied independently (decoupled). A variety of decoupled models developed and investigated at Natick have contributed directly to the coupled model presented in this paper. These studies include steady and unsteady CFD solutions about rigid decelerators

[1,2,3]. Unsteady CFD solutions about decelerators with a specified opening behavior have been investigated [4]. A dynamic spherical membrane model was developed at Natick [5]. This spherical membrane model was used in an early attempt to couple the structural dynamic code with a CFD code.

The logic required in coupling a CFD code to a structural dynamic code was established in stages of increasing complexity. All models described in this report are axisymmetric models. The first stage involves coupling a system of rigid disks connected by springs with the surrounding flow field. For example, a "payload" disk of small diameter and large mass was connected to a "decelerator" disk of large diameter and small mass by a linear spring. The equations for the coupled system were solved in time until a terminal velocity was reached. The relative motion of the disks damped out due to the coupled structural and aerodynamic effects. The second stage was to couple the dynamic spherical membrane model to the CFD model. For example, a hemispherical membrane was pinned along the skirt. The motion of the skirt was prescribed to start from rest and smoothly reach a steady "terminal" value. Ultimately, the aerodynamics about the membrane approached steady behavior. The dynamics of the spherical membrane naturally damped and the membrane approached a final nonspherical shape.

The present model involves coupling the CFD code to the MSD structural dynamic code representing a flat, circular solid-cloth parachute such as a C-9. This model was used in an attempt to predict the behavior of a quarter-scale C-9 canopy dropped from rest. The computational results will be compared with experimental results obtained by Dr. Calvin Lee of Natick [6]. This paper describes the coupled model and presents the computational results for the quarter-scale C-9. Future enhancements to the individual and coupled models are considered.

CURRENT MODEL

Coupling

The coupling approach used in the model is an explicit marching method in time. The CFD code is used as the main Fortran program, which calls the structural code subroutines. The coupled model starts the computations with the flow medium and structural components at rest. The CFD solver computes the pressure distribution for the flow field, which is zero everywhere for the first time step for these initial conditions. The pressure distribution over the surface of the structural model and the time step are sent to the structural code. The structural code integrates the equations of motion over this time step at a user-defined set of mass points. Each mass point coincides with a specific adjacent CFD vertex. The positions and velocities of the mass points are returned to and updated in the CFD code. These surface vertices in the CFD code are required to move with the motion specified by the structural code. The boundary condition imposed by the CFD code on these vertices represents a no-slip boundary condition. The CFD code computes the pressure distribution for the next time step and sends the surface differential pressure values and the time step to the structural code. The process continues by marching forward in time up to a specified completion time.

Computational Fluid Dynamics (CFD) Model

The SALE code is being employed as the flow solver in the current model [7]. SALE uses a finite difference algorithm to solve the time-dependent axisymmetric Navier-Stokes equation and conservation equations for mass and internal energy. The fluid pressure is determined from an equation of state. It should be noted that velocities are defined at the vertices of the computational grid, whereas pressures are defined at cell centers. The finite difference algorithm of SALE allows the use of nonuniform computational grids, made up of quadrilateral cells. This allows the grid to be deformed to model the curved surfaces of the decelerator.

SALE has the option of solving the Navier-Stokes equations for two-dimensional planar or axisymmetric coordinates. It utilizes the arbitrary Lagrangian-Eulerian (ALE) grid rezoning method, which allows the grid to be adjusted with time. This rezoning method is vital for solving flows about decelerators in motion or for inflation problems.

SALE uses a single block grid consisting of a network of quadrilateral cells. The mesh of cells is n_x cells wide and n_y cells high. For the current model, the decelerator surface is defined in the CFD grid by a set of adjacent, interior grid points. The computational grid consists of an interior "rezone" region which includes the decelerator grid points and an exterior region which is rectilinear and has a less dense grid structure than the "rezone" region. (See Figure 1.)

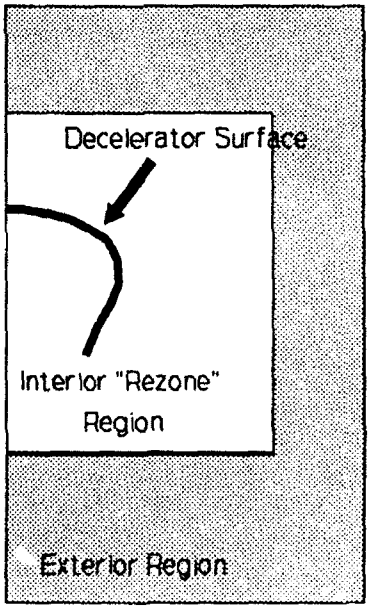

Figure 1. Computational Grid Structure

An initial grid is created by implicitly generating the interior "rezone" region and then extending the exterior region algebraicly from the outer boundary of the "rezone" region.

The interior "rezone" region is generated by deforming an initially uniform, rectangular grid so that appropriate cell vertices fit the desired decelerator shape. This gridding approach is demonstrated in Figure 2 where C is the grid vertex representing the skirt of the canopy and A represents the canopy apex.

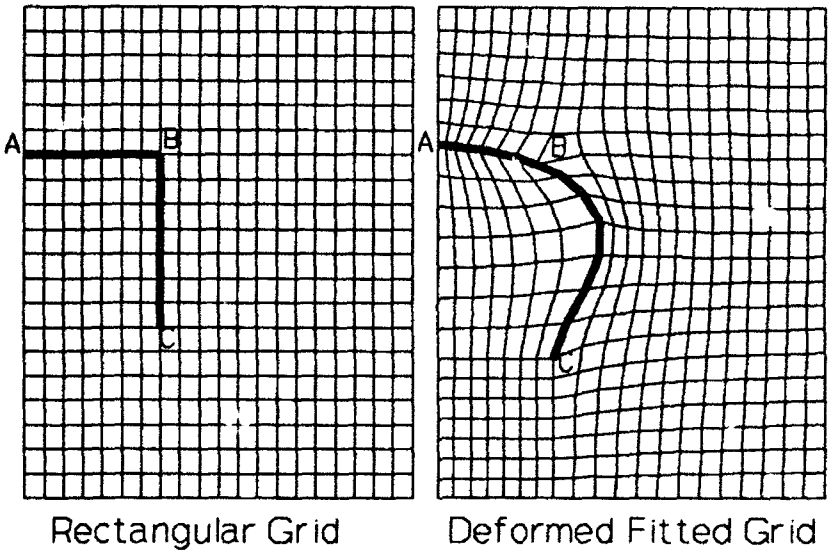

Figure 2. Interior "Rezone" Region of Computational Grid

The current model requires that the computational grid be modified each time step in order to fit the time-variant canopy shape. The interior "rezone" region of the grid is updated each time step with the same procedure that was used to create the initial grid. The exterior region is then updated to extend from the new distribution of grid points along the outer boundary of the "rezone" region. Once all grid points have been repositioned, the relative motion grid and the corresponding fluid is determined at each grid vertex.

The MSD model requires nodal pressure differences as input at all vertices on the canopy surface. Since SALE computes pressure values at cell centers, vertex pressures are defined as the average of the surrounding four cell pressures. Values for the surface pressures are then extrapolated from the two neighboring vertices. This process is done for both the inner and outer surface of the canopy. This is shown in Figure 3 where subscripts P1 and P2 are vertex pressures and P3 is the extrapolated nodal pressure on the upper surface of the canopy.

Point B is on the canopy surface at a corner in the CFD grid and often produces an adjacent cell which is quite distorted (see Figure 2). The result is a pressure distribution with a slight discontinuity at point B. For this reason, the differential pressure value sent to the MSD model at point B is evaluated by interpolation from a curve fitting the differential pressures at the surrounding vertices.

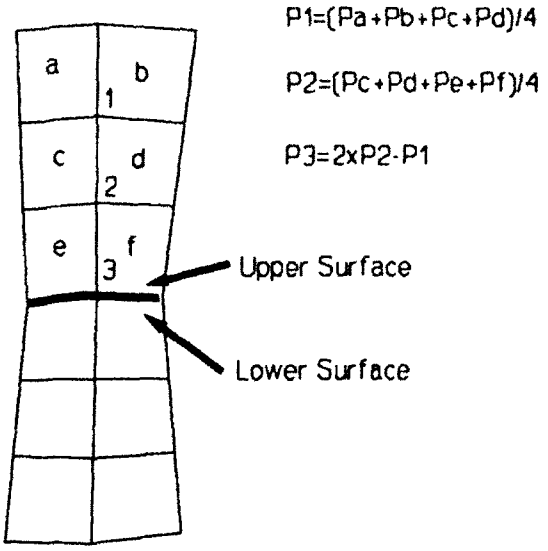

Figure 3. Surface Pressure Extrapolation

Mass Spring Damper (MSD) Model

The canopy is modeled as a series of lumped mass points connected by springs and dampers as shown in Figure 4. The MSD model fits into the overall coupled code as a set of Fortran subroutines. The MSD subroutines require a pressure distribution along the meridional length of the canopy and a time step as input. The program returns the position and velocity of each mass point at the requested time. The MSD model is being developed as a separate set of subroutines so that other parachute models could be used in its place or, so that it could be coupled with CFD codes other than SALE.

The MSD model is axisymmetric. It models flat circular solid cloth canopies such as a C-9. Newton's second law is applied at a user-defined number of mass points to obtain a set of coupled nonlinear differential equations. A free body diagram of a typical interior mass point is shown in Figure 5. The forces *F1*, *F2*, *F3*, *F4*, and *F5* applied to mass point *i* are described below.

- *F1* is the force predominantly due to the aerodynamic differential pressure acting across the canopy surface. It is the product of the current pressure difference over the canopy surface at mass point *i* and the current surface area associated with mass point *i*. (Note: A small amount of artificial normal damping is added in the normal direction to maintain numerical stability.)
- *F2* is the sum of the forces from the meridional spring and damper connecting mass points *i* and *i+1*. The spring force is the product of the spring constant and the change in length for mass points *i* and *i+1*. The spring force only acts when the distance between the mass points is greater than the constructed distance. The damping force opposes the relative velocity between mass points *i* and *i+1*. The force is the product of the damping constant and the relative change in velocity for mass points *i* and *i+1*. These dampers are required to damp out the high natural

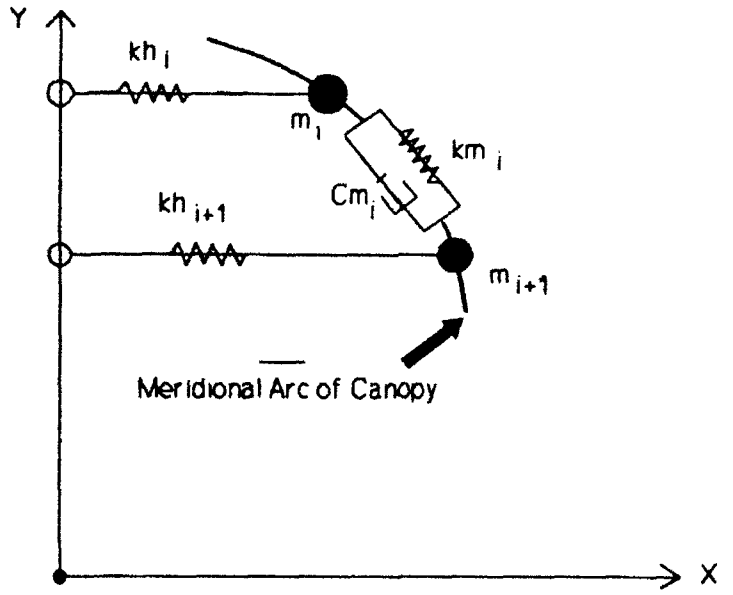

Figure 4. Mass Spring Damper Model

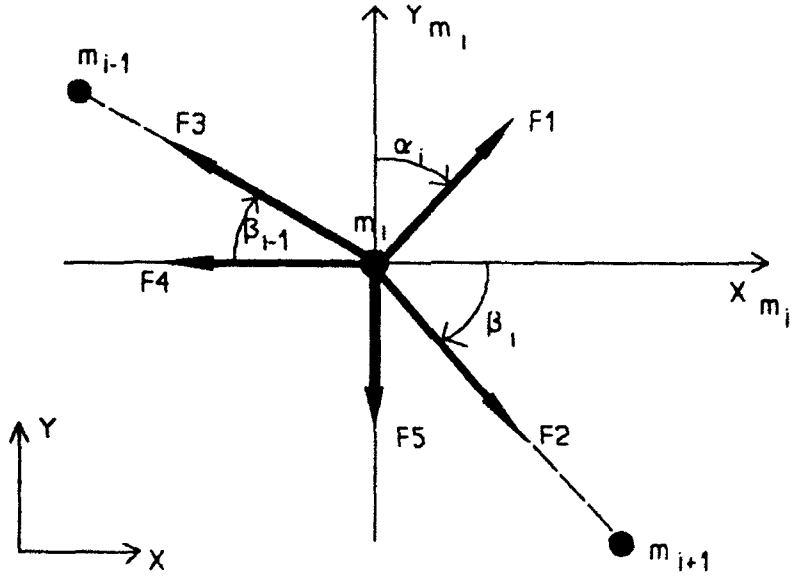

Figure 5. Free Body Diagram

frequencies in the meridional springs. These natural frequencies cause flow instabilities in connection with the "no-slip" boundary conditions at the canopy surface.

- *F3* is the sum of the forces from the meridional spring and damper connecting mass points *i* and *i-1*. Similar to *F2*.
- *F4* is the force from the "hoop" spring contribution. The "hoop" springs only engage when the current distance between the y axis of symmetry and the mass point *i* is greater than the

constructed meridional distance from the apex of the canopy to mass point *i*. The force is the product of the "hoop" spring constant and the positive quantity of deformation described above.
• *F5* is the force due to gravity on mass point *i*. This force is the product of the gravitational acceleration constant and the mass of mass point *i*.
The angles shown in Figure 5 are described below.
• α_i is the angle from the *y* axis to the outward normal direction associated with mass point *i*. The outward normal direction is calculated from the inverse of the first derivative of a third order Lagrange polynomial which passes through mass points *i-1*, *i*, and *i+1*.
• β_i is the angle from the local x axis of mass point *i* to the line segment connecting mass points *i* and *i+1*.

Applying Newton's second law to a typical interior mass point in the *x* and *y* directions results in the equations of motion shown in equations (1) and (2) below.

$$m_i\frac{d^2x_i}{dt^2}=P_i\sin\alpha_i+km_i\Delta l_i\cos\beta_i-$$
$$kh_i\Delta r_i-km_{i-1}\Delta l_{i-1}\cos\beta_{i-1}+ \qquad (1)$$
$$Cm_i\frac{d(\Delta l_i)}{dt}\cos\beta_i-Cm_{i-1}\frac{d(\Delta l_{i-1})}{dt}\cos\beta_{i-1}$$

$$m_i\frac{d^2y_i}{dt^2}=P_i\cos\alpha_i-km_i\Delta l_i\sin\beta_i+$$
$$km_{i-1}\Delta l_{i-1}\sin\beta_{i-1}-Cm_i\frac{d(\Delta l_i)}{dt}\sin\beta_i+ \qquad (2)$$
$$Cm_{i-1}\frac{d(\Delta l_{i-1})}{dt}\sin\beta_{i-1}-m_ig$$

These equations are reformulated into a set of first order ordinary differential equations (ODE's) that are nonlinear in space and first order in time. The equations are solved over the desired time step with initial conditions by utilizing the SLATEC ODE solver DDEBDF and associated subroutines [8]. The subroutine DDEBDF uses backwards differentiation formulas of orders one through five to integrate a system of first order ordinary differential equations.

Two half-gores and a radial are used to model the canopy as shown in Figure 6. The number of mass points used (a total of *n*) and the unstretched position of each mass point is user defined. The mass associated with each canopy mass point is based on the undeformed geometry of the canopy. The undeformed surface area for a mass point is multiplied by the undeformed

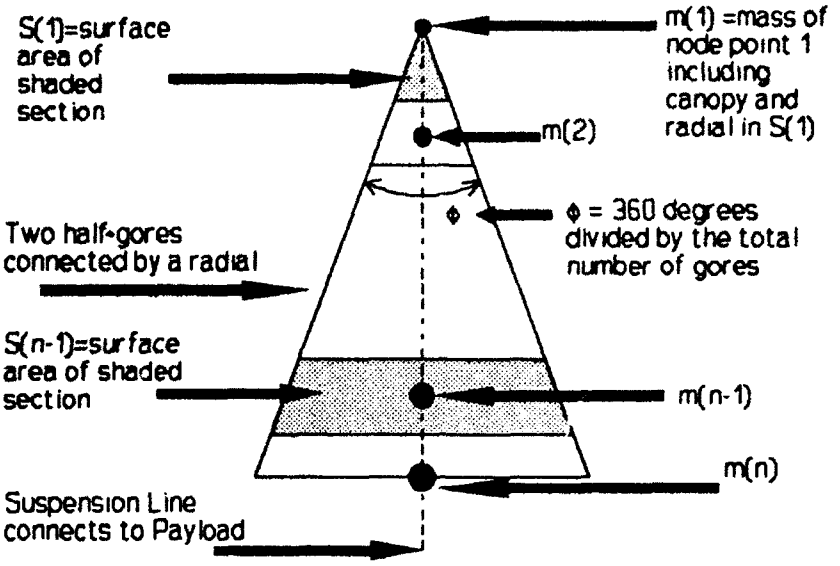

Figure 6. Layout for Two Half-Gores

thickness of the canopy fabric and the density of the canopy fabric. This quantity is added to the mass associated with the radial contribution to that mass point.

The meridional springs are modeled by assuming a linear force versus deflection curve for both the fabric and the radial. The material associated with a meridional spring is considered as a rectangular section as shown in Figure 7. The fabric spring and radial spring are considered to act in parallel. This approximation allows for the introduction of a Young's modulus term for

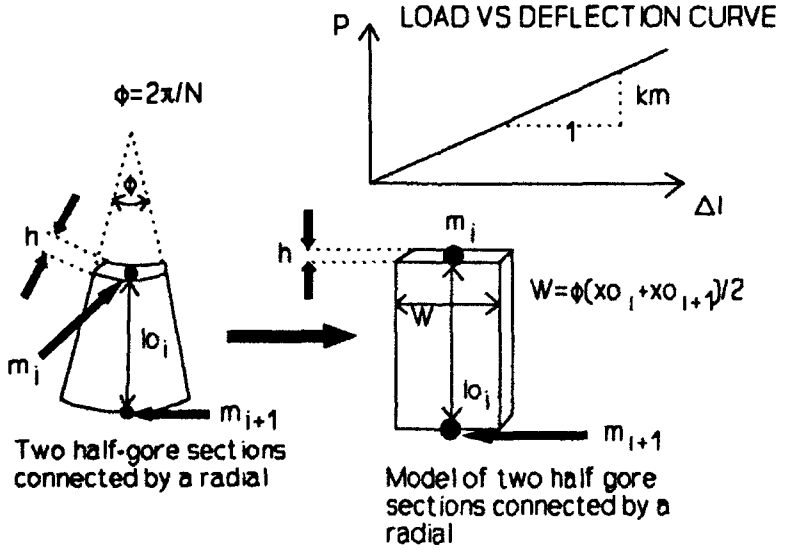

Figure 7. Meridional Spring Constants

both the canopy fabric and the radial. The equation to determine a meridional spring constant is shown in equation (3).

$$km_i = \frac{\pi E_2 h (xo_i + xo_{i+1})}{lo_i N} + \frac{E_1 A}{lo_i} \qquad (3)$$

The apex and skirt mass points on the canopy require special treatment due to different surface area calculations. The suspension line is modeled as a weightless spring connecting the skirt canopy mass point to the payload. The payload mass for the model is defined as the total payload mass divided by the number of gores in the model. The payload equation of motion is restricted to the *y* direction. Therefore, the total number of first order ODE's that are solved over each time step in the MSD model is equal to four times the total number of canopy mass points plus two.

The MSD model has many assumptions and is not expected to model a flat circular solid cloth canopy completely. However, the model is capable of modeling large deformations that are similar to those experienced by parachutes. The model is expected to yield a more accurate representation of a parachute with a variety of improvements that are discussed in a later section of this report.

PRELIMINARY RESULTS

The coupled computer model is being tested by modeling a quarter-scale C-9 solid-cloth canopy, which is dropped from rest. This choice was made because of the relatively simple set of initial conditions required and because the quarter-scale C-9 is currently being tested by Dr. Calvin Lee of Natick. The quarter-scale C-9 canopy is represented with 29 mass points along its canopy surface with a small degree of clustering towards the canopy apex. The total CFD grid is made up of 59 cells in the *x* direction and 104 cells in the *y* direction. The interior "rezone" region incorporated in the CFD grid has 44 cells in the *x* direction and 54 cells in the *y* direction (axis of symmetry). The canopy has a prescribed initial configuration, which provides a positive volume for all CFD cells.

The fluid and structural properties used in the computation are defined below. The fluid medium is air with standard atmospheric properties at sea level. The quarter-scale C-9 solid-cloth canopy has a constructed diameter of 7 feet and is made from 28 gores. The line length is 5.74 (feet) and the payload weight is 5.3 (pounds). The Young's modulus for the fabric and lines is taken as 30,000 (psf). The fabric thickness is 0.0004 (feet) and the line radius is 0.01 (feet). The gravitational constant is 32.2 (feet/second^2).

The initial shape of the canopy is unstretched. The shape is determined by defining the angle between the y axis and the suspension lines. The canopy skirt is required to remain tangent to the suspension lines for this initial configuration. The top of the canopy is required to trace

out a circular section so that the required total line length and canopy constructed diameter are consistent with a quarter-scale C-9 parachute. The initial payload position is defined as the origin of the y axis of symmetry.

The computation was run on a Kubota Titan 3000 mini-supercomputer. The entire computation took approximately 30 hours. The initial time step for the coupled computation was 1.0×10^{-6} seconds, which was permitted to grow to a maximum time value of 1.0×10^{-4} seconds. The computation ran to a completion time of four seconds.

The figures in Appendix A show the canopy shape at a sequence of times throughout the opening process. The initial configuration for the 29 canopy mass points and for the payload mass point is shown in Figure A-1. Figure A-1 also shows a sequence of canopy shapes for equally spaced time steps from the initial shape at time equal to zero seconds up to time equal to 0.6 seconds. Figures A-2 and A-3 are a continuation of Figure A-1 for times from 0.6 to 1.2 seconds and 1.2 to 1.8 seconds, respectively.

The predicted payload position and velocity curves as functions of time are shown in Figure 8. The predicted payload force versus time curve is shown in Figure 9. This force is calculated by taking the force in the suspension line spring that connects the payload mass point to the skirt mass point and multiplying its vertical component by the total number of gores. Even with the assumed initial shape and other approximations used in the model, this curve appears to be reasonable when compared to experimental data of Dr. Lee [6].

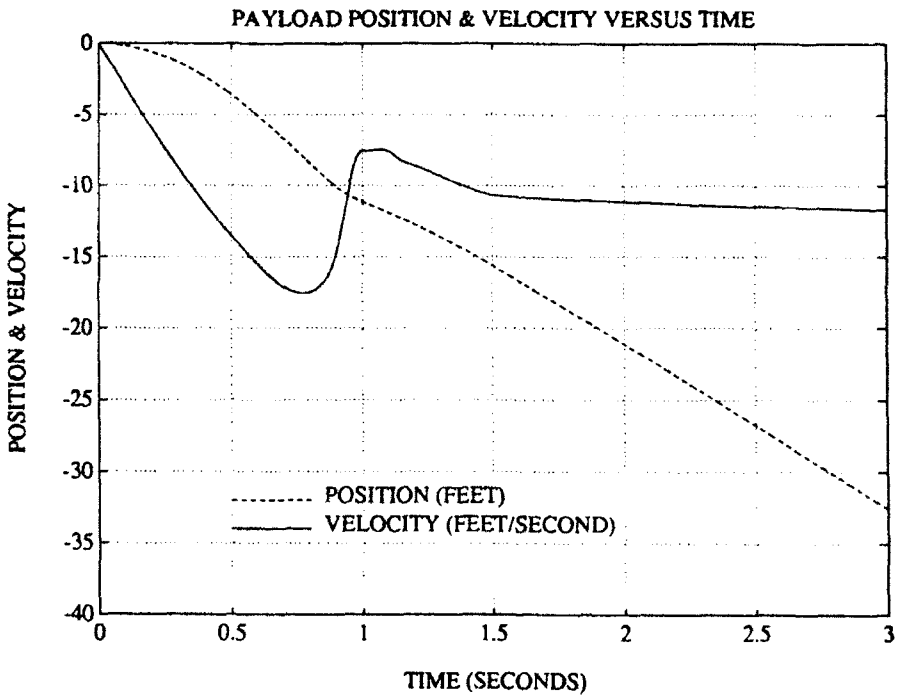

Figure 8. Payload Position and Velocity Versus Time

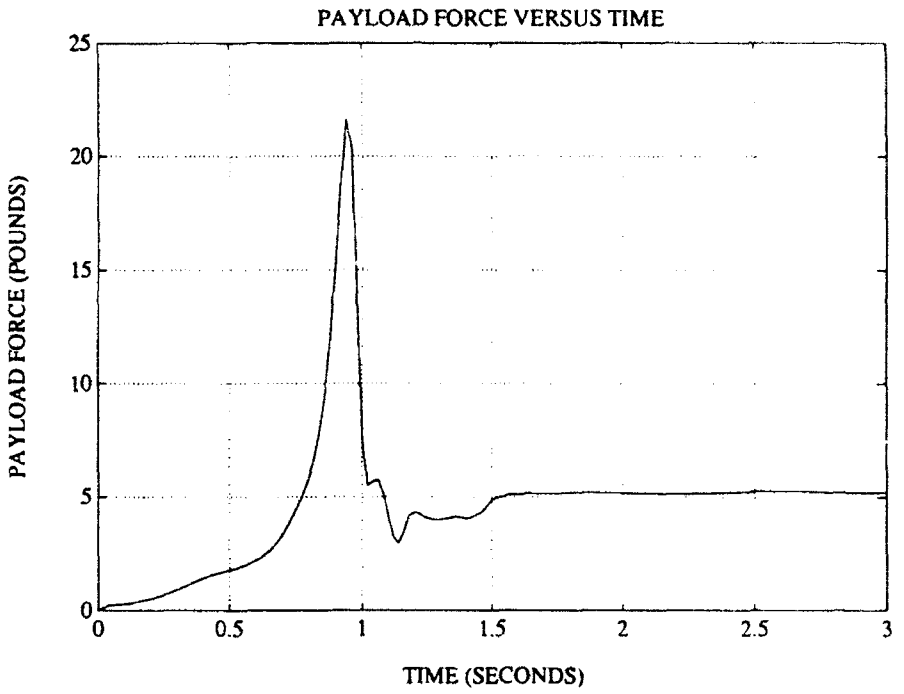

Figure 9. Payload Force Versus Time

A sequence of pressure and velocity fields for the interior "rezone" region of the CFD grid are shown in the figures in Appendix B. These plots are "snapshots" in time from 0.2 seconds to 2.4 seconds at 0.2 second increments. The pressure contour lines are shown on the left hand side of the figure. The canopy shape is highlighted by the pressure contour lines because of the discontinuity of the pressure field across the canopy surface. There are 41 contour lines. These contour lines range from a minimum value of -0.2 (psf) to a maximum value of 0.2 (psf) in 40 equal increments of 0.01 (psf) each. The right hand side of these figures show the velocity vectors. The velocity vectors are scaled equally for each snapshot to provide information on the time-dependent velocity field in a consistent manner.

A steady state solution is approached after the computation is run out to a real time of four seconds. The following values correspond to the final values at four seconds. The ratio of the projected diameter to the constructed diameter is 0.69. The ratio of the projected height to the projected diameter is 0.36. The terminal velocity is -12.0 feet per second. As expected, the vertical force transferred through the suspension lines to the payload is equal to the prescribed payload weight of 5.3 pounds.

FUTURE MODEL

Coupling

The current model is in its preliminary stage and there is significant room for improvement. The effects of various parameters have not yet been fully investigated. The explicit marching method should approach the exact solution to the coupled equations for a sufficiently small time step. However, an implicit method, which would require iterating between the structural and CFD codes, may be advantageous in the future. Another future requirement is the ability to model a larger variety of initial conditions.

CFD Model

One of the primary limitations of the current CFD model is its inability to represent canopy geometries early in the inflation phase. With the current model, such geometries result in highly distorted CFD grids. The accuracy of the CFD pressure field is adversely affected by such grids. In order to deal with canopy geometries early in the inflation process an alternate CFD gridding approach will need to be implemented. One option is to utilize a multigrid CFD method, which will allow grid points to be distributed about the canopy surface in a less distorted manner. One difficulty with the current CFD model is the extrapolation of pressure values to the canopy surface. This difficulty could be addressed with the implementation of a gridding method which results in orthogonality at the canopy surface. Such a gridding approach would result in a more accurate surface pressure distribution.

Another limitation of the current model is its exclusion of effective porosity. Previous research conducted by Dr. Earl Steeves at Natick addressed the effects of porosity on rigid decelerator problems. Porosity effects must be included in future models.

Mass Spring Damper (MSD) Model

The MSD model has room for substantial improvements. This section will discuss modifications that are presently being implemented and potential future modifications. The suspension line mass must be included in the model. This involves adding a user-defined number of mass points along the suspension line. These mass points will not coincide with vertices in the CFD model. The suspension line mass points will be connected by springs and dampers. The drag forces on the suspension lines will be included. The drag force on each line mass point is calculated using the current velocity vector of the mass point and the relative fluid velocity at the line mass point. The axisymmetric model can not include the flow disturbance caused by the suspension lines. Another necessary improvement to the MSD model involves the accuracy of the hoop force. The hoop contribution to mass point loadings may be best incorporated into the model by applying the appropriate logic used in the CALA code [9]. The model should include canopy contact effects, a Poisson's ratio effect for the canopy fabric, and the nonlinear material properties of the fabrics and lines that are used in parachute construction.

The force due to the pressure difference across the canopy surface needs to be of a higher order of accuracy. The pressure should be assumed as a piecewise linear function and integrated between mass points along the canopy length to obtain a more accurate force contribution at each mass point. Various reefing condition options will be included in the model. For example, skirt reefing will be modeled by restricting the x deflection of the skirt mass point either for a specified quantity of time or until a specified payload velocity has been obtained. Another major addition will be to include other canopy geometries such as conical, flat extended skirt, and annular canopies. The ribbon canopy presents a larger challenge and may need to be modeled as a solid canopy with an appropriate quantity of porosity. The number of mass points required to model each ribbon individually would result in an excessive number.

Eventually a higher-order three-dimensional model, most likely of a finite element type, must be developed in connection with a three-dimensional CFD code.

CONCLUSIONS

The complexity of modeling the opening process stems from the coupling between the structural dynamics of the canopy, lines plus payload and the aerodynamics of the surrounding fluid medium. This paper has described ongoing research at Natick which involves the coupling of a CFD code and a structural dynamics code. The solution to the c upled problem is expected to assist in the development of future U.S. Army airdrop systems, which include the capability of deploying at low altitudes and high speeds. Initial computational results with the current model described in this paper compare favorably with experimental data for a quarter-scale C-9. Future computational models are expected to provide significant insight about the behavior of parachutes during the opening process.

This document reports research undertaken at the US Army Natick Research, Development and Engineering Center and has been assigned No. NATICK/TR-93/029 in the series of reports approved for publication.

REFERENCES

1. Steeves, Earl C. "Prediction of Decelerator Behavior Using Computational Fluid Dynamics." *Proceedings of AIAA 9th Aerodynamic Decelerator and Balloon Technology Conference.* Albuquerque, NM. October 7-9, 1986.

2. Steeves, Earl C. "Analysis of Decelerators in Motion Using Computational Fluid Dynamics." *Proceedings of AIAA 10th Aerodynamic Decelerator and Balloon Technology Conference.* Cocoa Beach, FL. April 18-20, 1989.

3. Stein, Keith R. "Computations of the Flow Characteristics of Aerodynamic Decelerators Using Computational Fluid Dynamics." *Proceedings of AIAA 11th Aerodynamic Decelerator and Balloon Technology Conference.* San Diego, CA. April 9-11, 1991.

4. Stein, Keith R. "An Investigation of Parachute Aerodynamic Characteristics Using Computational Fluid Dynamics." *Proceedings of the 4th Natick Science Symposium.* Natick, MA. June 9-10, 1992.

5. Benney, Richard J. "A Nonlinear Dynamic Spherical Membrane Model." U.S. Army Natick Research, Development and Engineering Center. Natick Technical Report No. NATICK/TR-93/017. January 1993.

6. Lee, C.K. "Modeling of Parachute Opening: An Experimental Investigation." *Journal of Aircraft.* Vol. 26, No. 5. May 1989.

7. Amsden, A.A., Ruppel, H.M., and Hirt, C.W. "SALE: A Simplified ALE Computer Program for Fluid Flow at All Speeds." Los Alamos Scientific Laboratory Report No. LA-8095, 1980.

8. SLATEC Library, A collection of FORTRAN mathematical subprograms available through the National Energy Software Center (NESC)

9. Sunberg, W.D. "New Solution Method for Steady-State Canopy Structural Loads." *Journal of Aircraft.* Vol. 25, No. 11. November 1988.

APPENDIX A.

Canopy Shape Versus Time

APPENDIX A

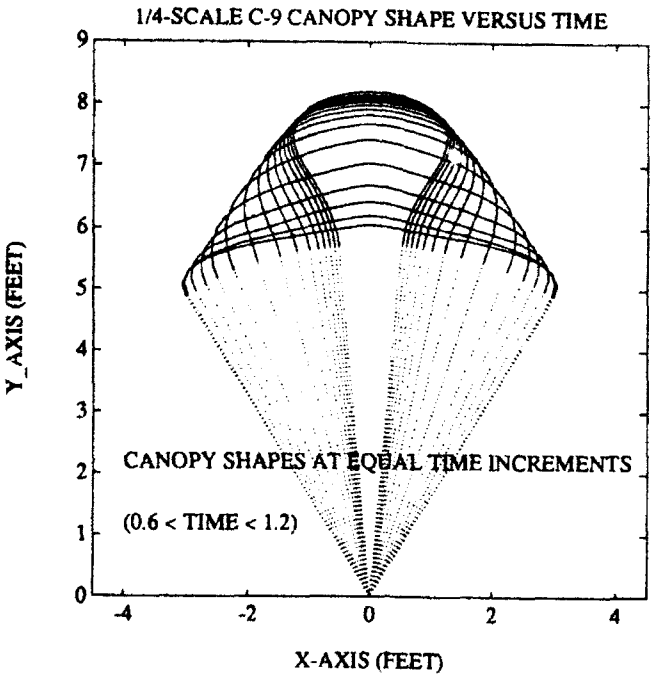

Figure A-1. Canopy Shape Versus Time in Seconds (0.0<t<0.6)

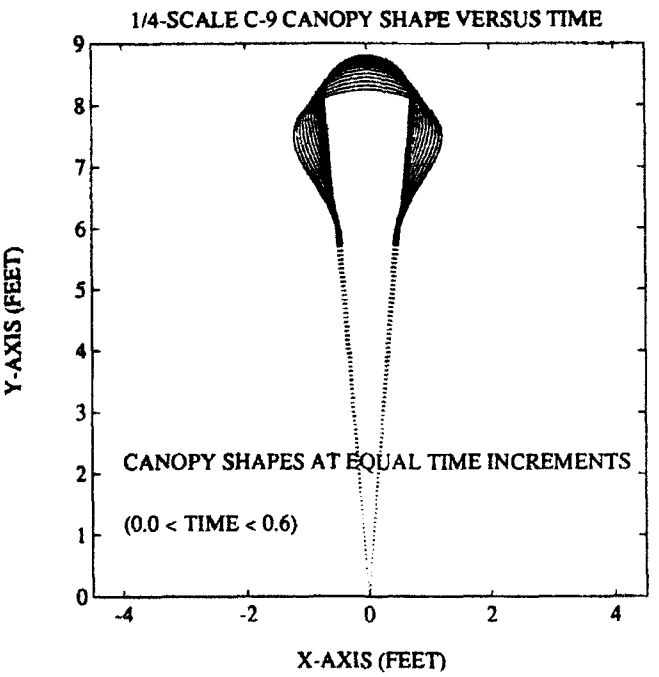

Figure A-2. Canopy Shape Versus Time in Seconds (0.6<t<1.2)

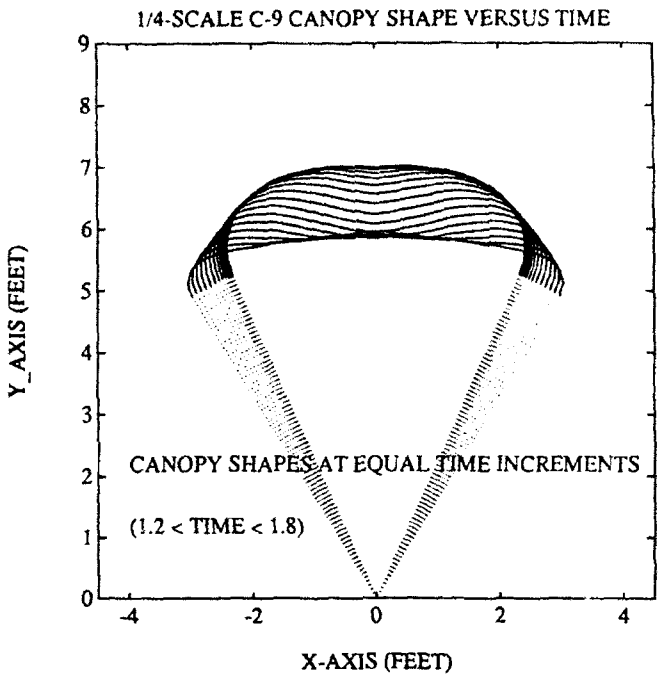

Figure A-3. Canopy Shape Versus Time in Seconds (1.2<t<1.8)

APPENDIX B.

CFD Flow Field Versus Time

APPENDIX B
(Pressure Contours and Velocity Field)

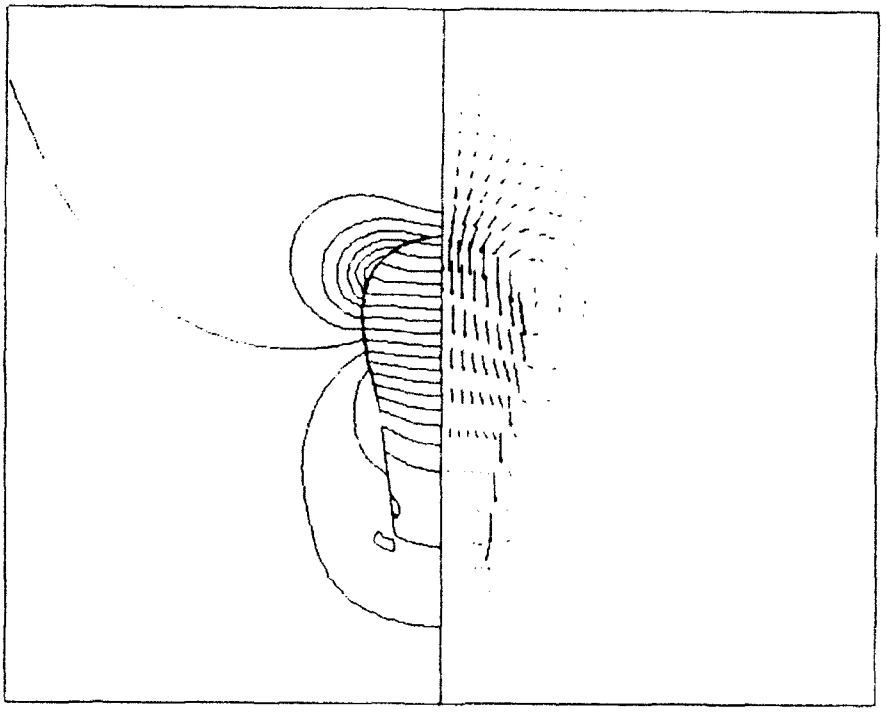

Figure B-1. CFD Solution (t=0.2 seconds)

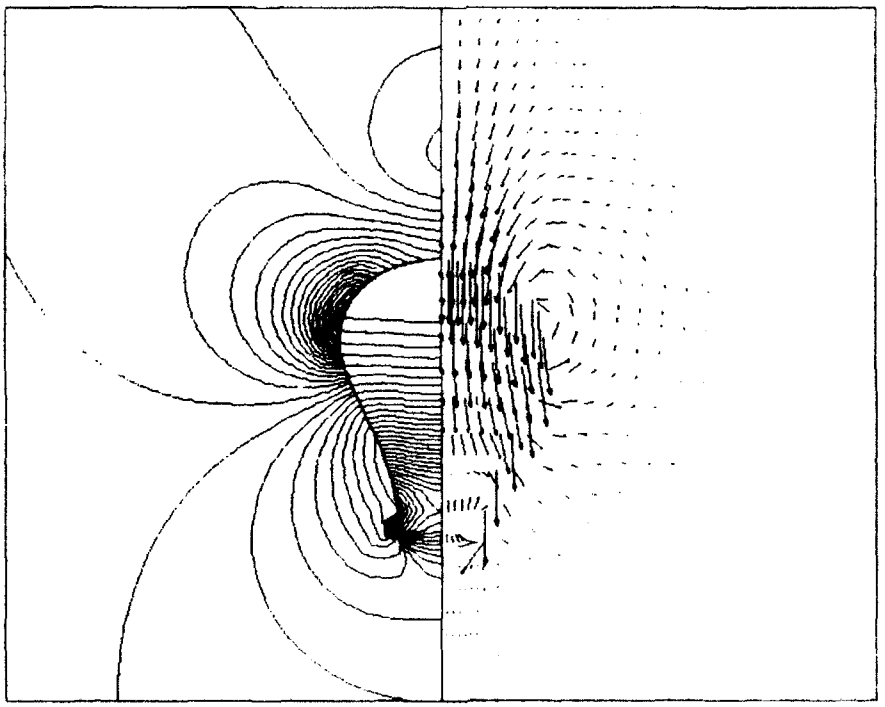

Figure B-2. CFD Solution (t=0.4 seconds)

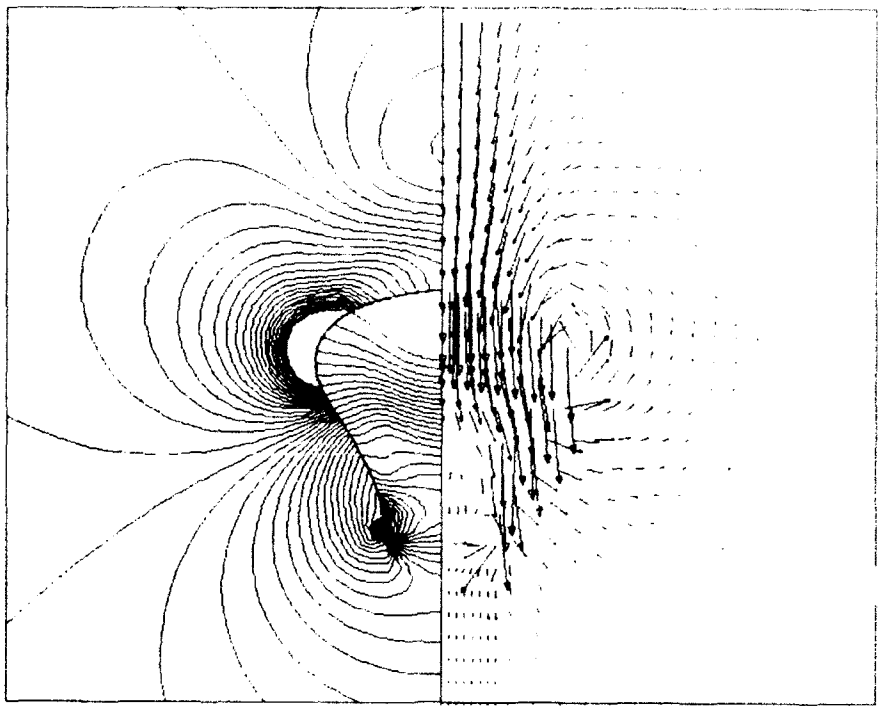

Figure B-3. CFD Solution (t=0.6 seconds)

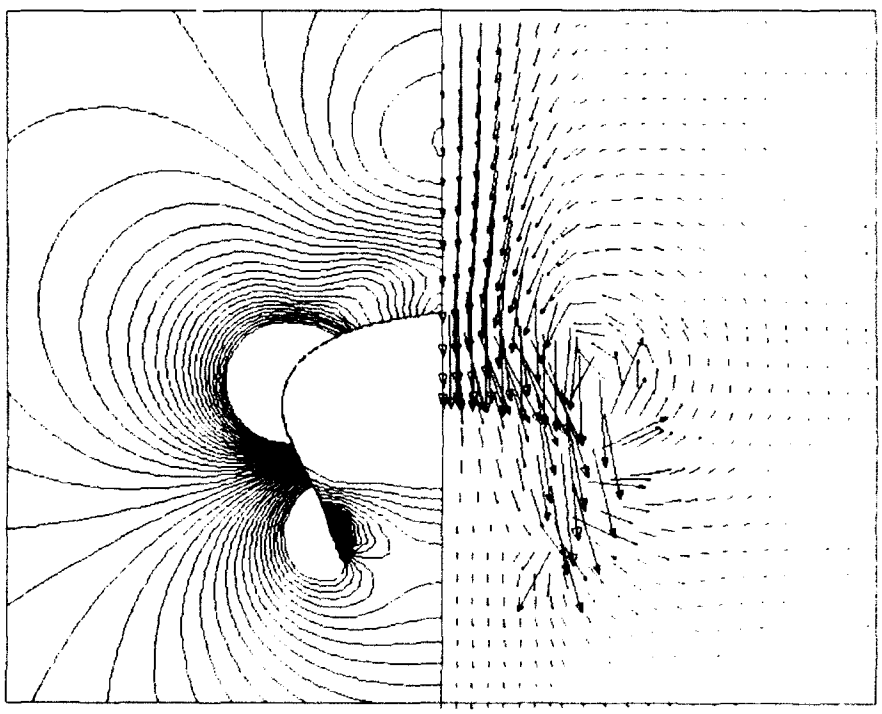

Figure B-4. CFD Solution (t=0.8 seconds)

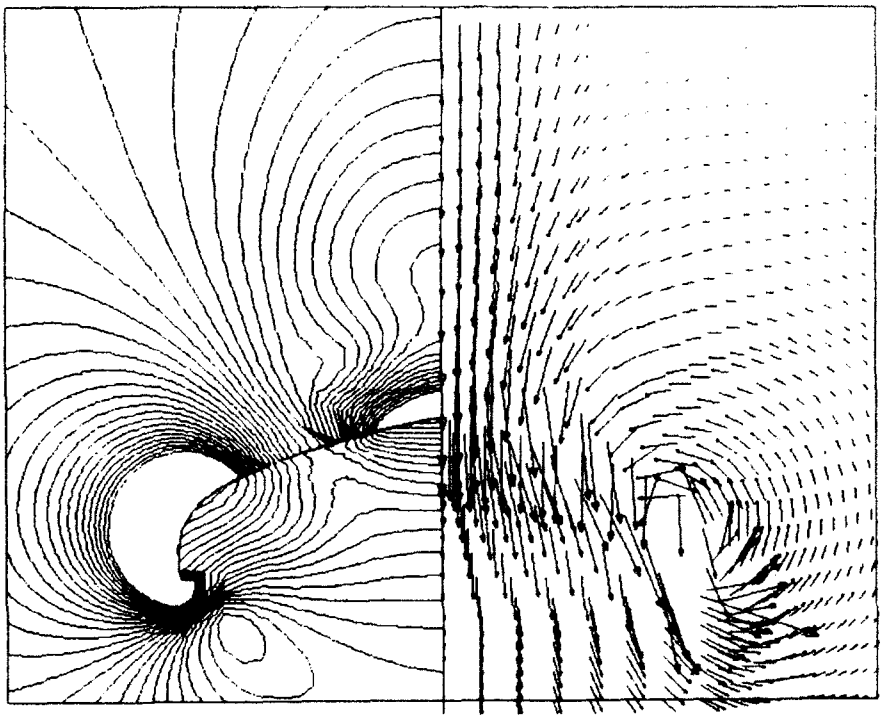

Figure B-5. CFD Solution (t=1.0 seconds)

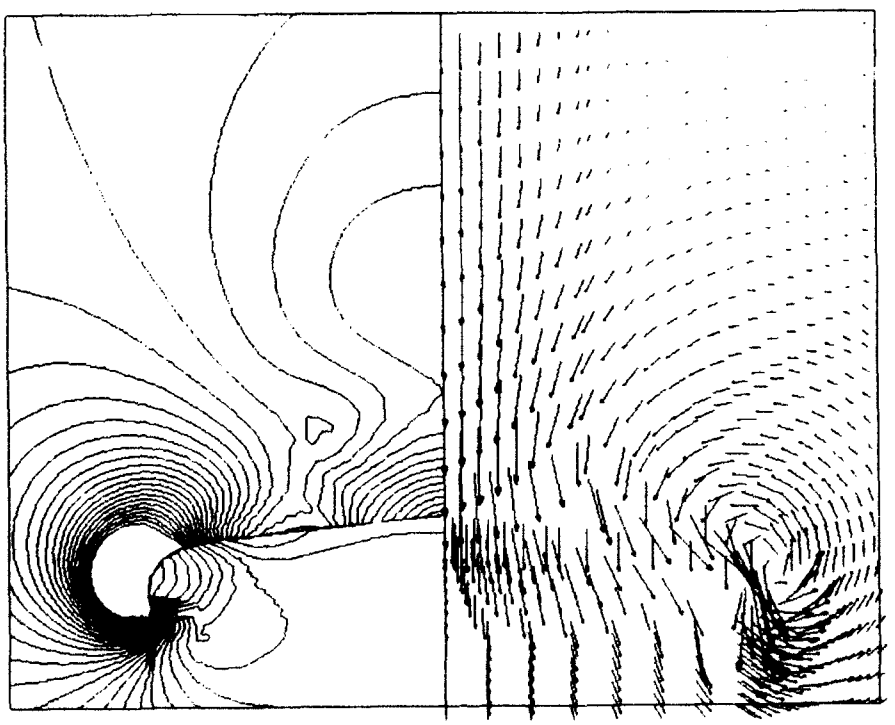

Figure B-6. CFD Solution (t=1.2 seconds)

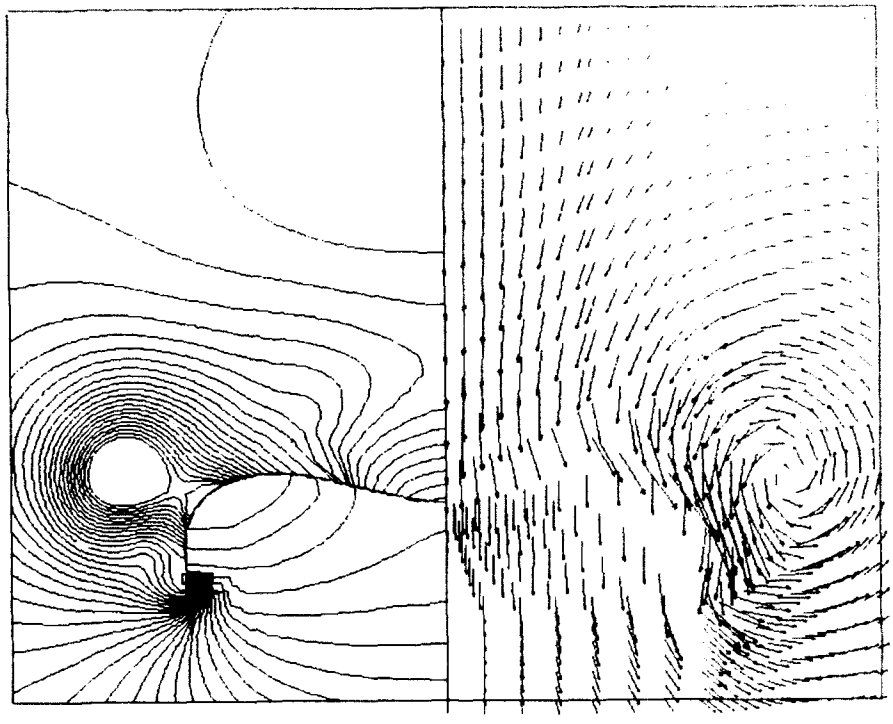

Figure B-7. CFD Solution (t=1.4 seconds)

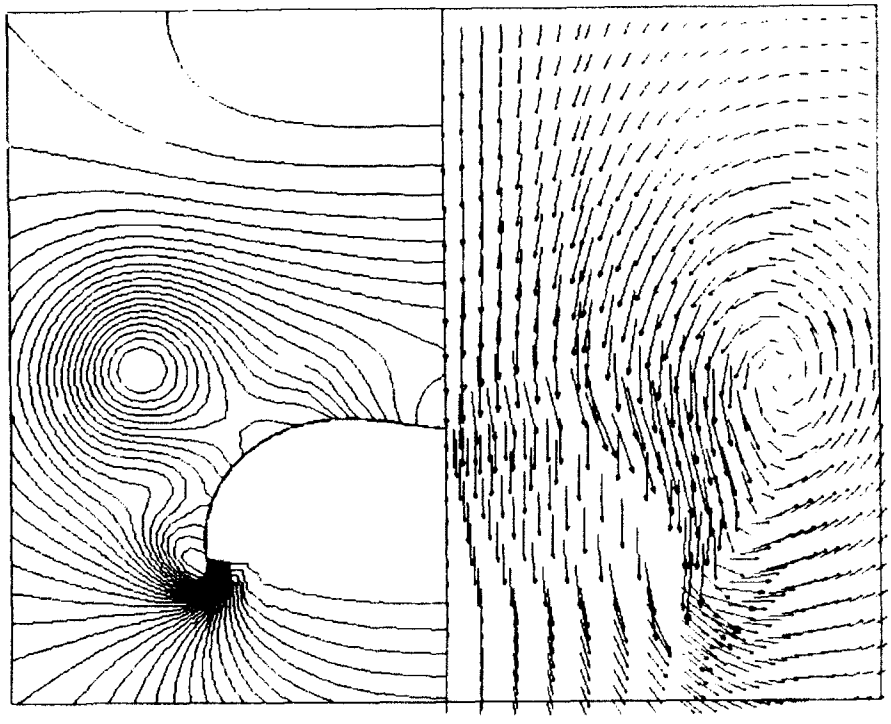

Figure B-8. CFD Solution (t=1.6 seconds)

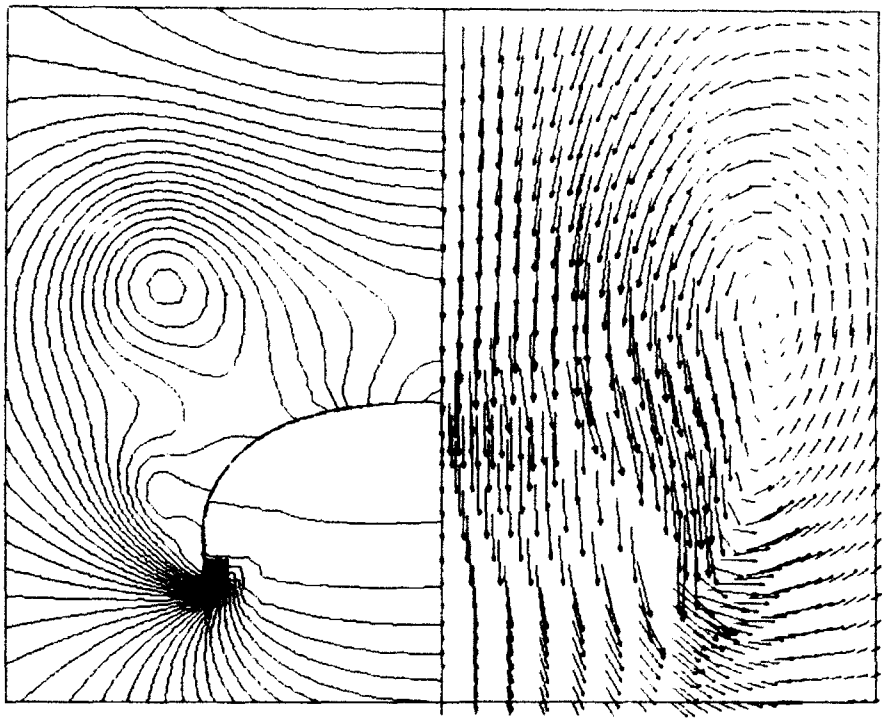

Figure B-9. CFD Solution (t=1.8 seconds)

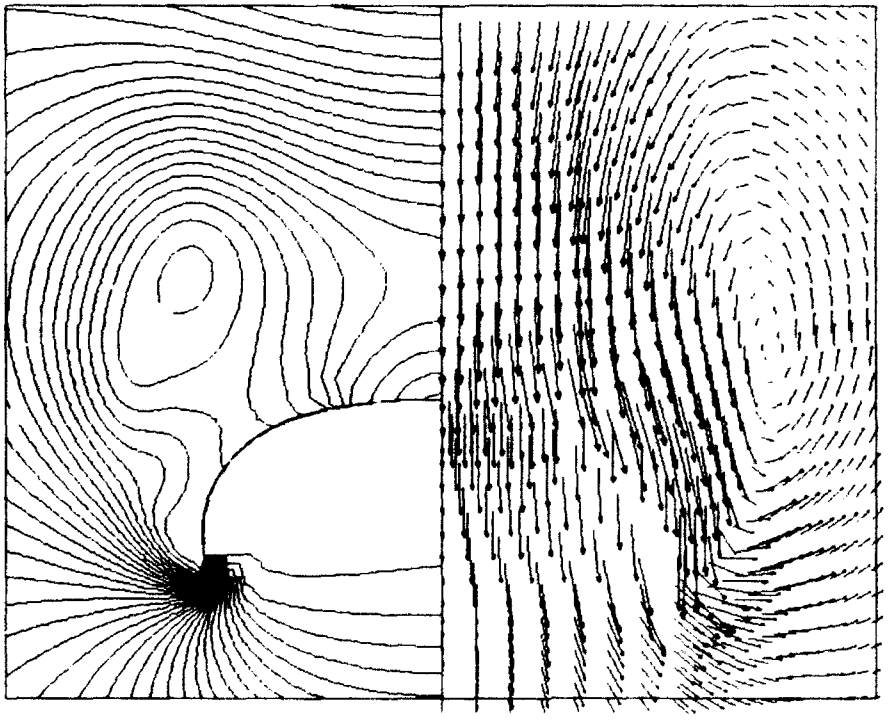

Figure B-10. CFD Solution (t=2.0 seconds)